

## BASIC FEATURES OF SENSORY NEURONS FROM DORSAL ROOT GANGLIA IN TCR-HA<sup>+/-</sup>/RIP-HA<sup>+/-</sup> MICE

BEATRICE MIHAELA RADU<sup>\*</sup>, ADINA DANIELA IANCU<sup>\*\*</sup>, ADELA MARIN<sup>\*</sup>, M. RADU<sup>\*\*\*</sup>,  
D.D. BANCIU<sup>\*</sup>, CRINA STAVARU<sup>\*\*</sup>, D.L. RADU<sup>\*\*</sup>

<sup>\*</sup>Department of Animal Physiology and Biophysics, Center of Neurobiology and Molecular Physiology, Faculty of Biology, University of Bucharest, 91–95, Splaiul Independenței, Bucharest, 050095, Romania, beatrice\_macri@yahoo.com

<sup>\*\*</sup>Laboratory of Cellular Immunity, “Cantacuzino” National Institute for Microbiology and Immunology, 103, Splaiul Independenței, Bucharest, 050096, Romania

<sup>\*\*\*</sup>Department of Health and Environmental Physics, “Horia Hulubei” National Institute for Physics and Nuclear Engineering, PO Box MG6, Măgurele, 077125, Romania

*Abstract.* Despite the increased prevalence of peripheral diabetic neuropathy, some of its mechanisms are still unknown. In our study, we have used a double transgenic mice (dTg) model, TCR-HA<sup>+/-</sup>/RIP-HA<sup>+/-</sup>, which develops a fulminating type of insulin-dependent diabetes. The goal of our study was to reveal the molecular mechanisms of diabetic neuropathy in neuronal primary cultures. The presence of the transgenes, that are responsible for the etiopathogenesis of type I diabetes, is determined by the PCR technique. Blood glucose, insulin level and corporal weight are monitored after 4 weeks of life. Neuronal primary cultures are dissociated from dorsal root ganglia. Electrophysiological recordings of these neurons are performed by patch-clamp technique, whole-cell configuration. In our study we have recorded the characteristics of the action potential and the hyperpolarization activated currents in sensory neurons. Significant differences were evidenced between the electrophysiological profiles of the sensory neurons from dorsal root ganglia dissected from TCR-HA<sup>+/-</sup> / RIP-HA<sup>+/-</sup> mice compared to BALB/c mice.

*Key words:* type I diabetes, sensory neurons, action potential,  $I_h$  current.

### INTRODUCTION

Diabetic neuropathy is the most common form of peripheral neuropathy in the developed world, affecting approximately 30–60% of all diabetic patients. The most common peripheral neuropathies are sensorial, in which patients experience altered sensory perception [4]. The underlying mechanisms are complex and not completely understood [15]. However, it is generally accepted that degeneration of

---

Received March 2009;  
in final form March 2009.

unmyelinated C-fibers and A $\beta$ -fibers is an initiating factor [7, 15]. Damage to C-fibers causes increased excitability via upregulation of Na<sup>+</sup> channels and  $\alpha$ -adrenergic receptors [8, 11, 13]. Pain sensitisation is further enhanced in the dorsal horn by excitotoxic stimulation of nociceptive interneurons by collaterals from A $\beta$ -fibers, so-called central sensitization [15, 20].

Symptoms of diabetic peripheral neuropathy include progressive loss of thermal and tactile pain sensation [3, 27]. However, most individuals with diabetic neuropathy experience reduced perception, a fraction (~10%) experience painful symptoms [3]. Altered pain sensation is partly due to some changes in TRPV1 expression. In STZ-induced diabetic mice it has been shown that increased thermal sensitivity results from sensitization of TRPV1, possibly through PKC [6, 12, 14].

In diabetic rats with hyperalgesia, dorsal root ganglion (DRG) neurons display increased frequency of action potential generation in response to sustained suprathreshold mechanical stimulation [1, 9, 18] and increased spontaneous activity.

Several animal models for diabetes are described in the literature: classic surgical model of type I diabetes – total pancreatectomy [26], pharmacologically induced diabetes by agents that selectively destroy the pancreatic cells, such as streptozotocin or alloxan [9, 18], spontaneous models of type I diabetes – BBDP and NOD mouse [21]. Compared to the above described models, the double transgenic mice TCR-HA<sup>+/-</sup>/RIP-HA<sup>+/-</sup> is a genetic model that corresponds to the clinical features of type I diabetes and that is characterized by fulminate evolution of the disease.

In this paper, we present the basic features of the sensory neurons from dorsal root ganglia dissected from double transgenic mice versus normal mice.

## MATERIALS AND METHODS

### ANIMALS

Two murine strains were used in our study: BALB/c and TCR-HA<sup>+/-</sup>/RIP-HA<sup>+/-</sup> mice. Progeny were obtained from the mating of BALB/c mice-expressing transgenes encoding a TCR recognizing an immunodominant epitope of influenza PR8 virus hemagglutinin (HA110–120) in association with I-Ed (TCR-HA<sup>+/-</sup>), and B10.D2 mice expressing the PR8 influenza virus HA transgene (RIP-HA<sup>+/-</sup>, [24]). Two strains were obtained upon mating: double transgenic mice (TCR-HA<sup>+/-</sup>/RIP-HA<sup>+/-</sup>, [2, 23]) that develop type I diabetes by an autoimmune mechanism and single transgenic mice (TCR-HA<sup>-/-</sup>/RIP-HA<sup>+/-</sup>) that are non-diabetic descendants.

In our study we have used 22 BALB/c mice and 20 dTg diabetic mice. All the electrophysiological data were acquired at the age of 14 weeks.

#### SENSORY NEURONS PRIMARY CULTURE

The animal is anesthetized by CO<sub>2</sub> inhalation for approximately 1 min. It is decapitated and upon removing the spinal cord, the dorsal root ganglia are removed. An enzymatic treatment (1 mg/mL collagenase and 1 mg/mL dispase) is applied to the ganglions during 1 h at 37 °C. The enzymes are inactivated with Dulbecco's modified Eagle's medium (DMEM F-12; Sigma Aldrich) supplemented with 10 % horse serum (Sigma Aldrich). Upon gentle trituration and centrifugation (900 × g, 10 min, 25°C), the dissociated neurons are deposited on Petri dishes pre-treated with poly-D-lysine, and after 1h incubation they are supplemented with DMEM F12 + 10% horse serum. Neurons are maintained in culture 1–3 days prior to patch-clamp recordings.

#### ELECTROPHYSIOLOGY PROTOCOLS

Patch clamp pipettes were pulled from borosilicate glass capillaries (GC150F-10, Harvard Apparatus Ltd., Edenbridge, UK) with a microprocessor-controlled vertical puller (PUL-100, WPI, Sarasota, FL), then fire-polished under a microscope to a final resistance in the range 3–5 MΩ for whole-cell recordings. Cells cultured in Petri dishes were kept at 25 °C with a Peltier-driven temperature controller placed on the recording microscope stage (TC202A, Harvard Apparatus). Solutions were delivered via a self-built low-dead volume fast exchange system (switching time 100 ms) with the tip placed at approximately 100 μm from the cell, at a constant flow rate of 0.3 mL/min. The electrical signals were converted and/or amplified with a WPC-100 amplifier (ESF electronic, Göttingen, DE), hardware filtered at 3 kHz for whole-cell recordings, sampled with a Digidata 1200B acquisition board (Axon Instruments, Foster City, CA) under pClamp 8.1 in gap-free mode and stored on hard-disk. The sampling intervals were 1 ms for whole-cell recordings, and the holding potential in voltage clamp mode is –60 mV.

The  $I_h$  currents were evoked by a series of hyperpolarizing pulses presented from a  $V_H$  of –60 mV (10 mV per step to a final potential of –110 mV; 500 ms, 4 s interstimulus interval). A 10 ms, 1000 pA current step was used to evoke the action potential. The bath solution consisted of (in mM): NaCl 140, KCl 4, CaCl<sub>2</sub> 2, MgCl<sub>2</sub> 1, HEPES 10, pH 7.40 at 25 °C with NaOH. The bath solution also contained freshly added 10 mM glucose. The pipette solution contained (in mM): NaCl 10, KCl 120, CaCl<sub>2</sub> 1 / BAPTA 10, MgCl<sub>2</sub> 3.45, HEPES 10, pH 7.20 at 25 °C with KOH.

#### GENOTYPING

The following primers were used under standard conditions for PCR: for the TCR-HA transgene, forward primer 5'-TAG GAGAAAGCAATGGAGAC-3' and reverse primer 5'-GTACCTGGTATAAACAACACTCAG-3'; for the HA transgene, forward primer 5'-GTCCTACATTGTAGAAACA-3' and reverse primer 5'-GTGACTGGGTGTATATTCT-3'. After amplification, the migration was done in an agarose gel electrophoresis, at 100 mV for 30 minutes. A weight marker (72 – 1353 bp) was used and the gels were photographed under UV transillumination.

#### DIABETES MONITORING

Blood samples were collected at 1-week intervals beginning at 4 weeks of age. Plasma glucose concentrations were measured with a OneTouch Ultra monitor (LifeScan). Simultaneously, the glycosuria was measured with Uristick strips and the body weight was also monitored. Insulin level was measured by ELISA method (Tecan) by Mouse Insulin ultrasensitive ELISA kit (DRG Instruments GmbH, Germany).

#### STATISTICAL ANALYSIS

Data were analysed with Clampfit 9.0 (Axon Instruments) and Sigmaplot 6.0 (SPSS Inc. Chicago, USA). Significance of differences between various groups of mice was determined by Student's t test, the number of cells analyzed for each mice group being mentioned in each graph as *n*. Differences were considered to be statistically significant when P values were < 0.05, see the \* in graphs. The graphs were created using Origin Pro 8.0 (OriginLab Corporation, USA).

### RESULTS AND DISCUSSIONS

#### BLOOD AND BODY PARAMETERS OF THE ANIMAL MODEL

Numerous animal models have been developed to mimic diabetes. The diabetic syndrome in BBDP (*Bio Breeding Diabetes Prone*) rats closely resembles insulin-dependent, ketosis-prone type I diabetes mellitus in humans, and is characterized by hyperglycemia, lymphocytic insulinitis, and the presence of antibodies to islet cell-surface molecules. A major distinguishing feature is a genetically transmitted, lifelong lymphopenia characterized by elevated numbers of natural killer cells and depressed numbers of T-helper and T-suppressor cells.

BBDP rats are prone to several of the long-term complications of diabetes, in particular the neuropathy and retinopathy [21]. NOD (*non-obese diabetes*) mice develop an autoimmune lesion involving lymphocytic infiltration and destruction of the pancreatic cells, which leads to hypoinsulinemia, hyperglycemia, ketoacidosis, and death [19]. These mice are particularly well suited for genetic and immunologic studies, as well as for research on environmental factors that influence the expression of diabetes.

Beside these autoimmune diabetes models, another model is the TCR-HA<sup>+/-</sup>/RIP-HA<sup>+/-</sup> mice. In this case, around two to three weeks after birth can be observed a rather strong accumulation of lymphocytes around the pancreatic islets, but the mechanism is rather different from that in NOD mice. Insulin-dependent diabetes mellitus results from the autoimmune destruction of the insulin-producing cells of the pancreatic islets.

This last model was used in the present study. Genotyping of mice was done using PCR, where the product obtained from RIP-HA Tg mice was 670 bp, the product obtained from TCR-HA Tg mice yielded a product of 351 bp, whereas dTg mice revealed both 670 bp and 351 bp in length (Fig. 1).

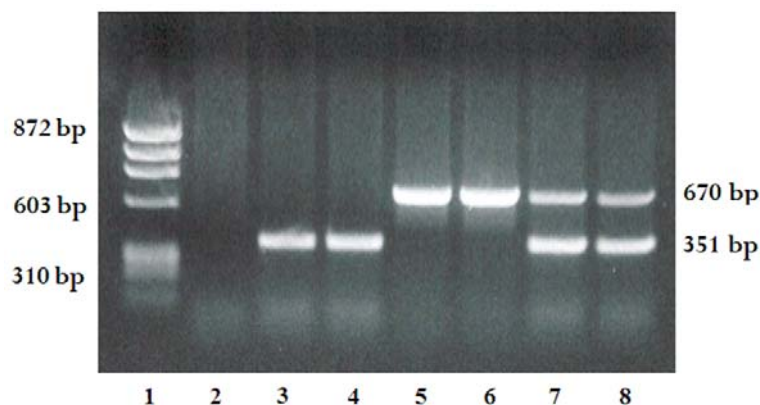


Fig. 1. Genotyping of mice by PCR. Lane 1, marker (DX174 RFDNA/HaeIII fragments, 72-1353 bp). Genomic DNA was used as template from BALB/c mouse (lane 2 shows the absence of transgenes), TCR-HA transgenic mice (lane 3 and 4 show the presence of TCR-HA transgenes), RIP-HA transgenic mice (lane 5 and 6 show the presence of HA transgenes) and double transgenic mice (lane 7 and 8 show the presence of both transgenes).

The TCR-HA<sup>+/-</sup> / RIP-HA<sup>+/-</sup> mice have a body weight more reduced than BALB/c mice until the 10<sup>th</sup> week (Table 1). During the first 10 weeks, the body weight increases both for dTg diabetic mice and for BALB/c mice, and between the 10<sup>th</sup> and the 14<sup>th</sup> week the body weight almost equalises. The glycemia of the dTg diabetic mice is higher than > 200 mg/dL, and has more elevated values than those corresponding to BALB/c mice. The glycosuria level is well correlated with

glycemia level, its values being very high for diabetic mice compared to normal mice. Between the 2<sup>nd</sup> and the 4<sup>th</sup> week, the insulin level decreases for the dTg diabetic mice compared to BALB/c mice. All these characteristics are critical for the installation of the hyperglycemic condition, and there are essential features that reproduce the clinical key points of diabetes.

These blood and body parameters were monitored permanently between 2<sup>nd</sup> to 4<sup>th</sup> week (insulin level) and between 4<sup>th</sup> and 14<sup>th</sup> week (body weight, glycemia level and glycosuria level). For the electrophysiological recordings, we have used only the mice that survived until the 14<sup>th</sup> week, and that already had 10 weeks since hyperglycemic condition was installed. Taking into account the data from the literature that suggested the nerve damage as a consequence of 10 weeks exposure at hyperglycemia [25], we have considered that the mice from our model (at the age of 14 weeks) are well suited for testing the sensory excitability properties.

Table 1

Characteristics of the animal model: body weight and glycemia, glycosuria and insulin level for dTg diabetic mice vs normal mice

	week	Body weight (g)	Glycemia level (mg/dL)	Glycosuria level (mg/dL)	Insulin level (ng/L)
BALB/c mice	II	–	–	–	0.69 ± 0.23
	III	–	–	–	0.88 ± 0.28
	IV	14.00 ± 0.73	177.50 ± 15.71	3.30 ± 0.78	0.67 ± 0.22
	V	16.12 ± 0.88	146.43 ± 24.28	1.37 ± 0.45	–
	VI	17.75 ± 1.06	154.43 ± 20.73	–	–
	VII	18.31 ± 0.87	108.25 ± 5.05	–	–
	VIII	18.75 ± 0.93	135.00 ± 5.65	–	–
	IX	19.96 ± 0.99	116.00 ± 9.08	–	–
	X	20.43 ± 1.09	122.37 ± 10.92	–	–
	XI	21.06 ± 1.06	112.20 ± 33.81	–	–
	XII	21.18 ± 0.27	109.80 ± 2.48	–	–
	XIII	21.62 ± 0.25	105.20 ± 8.40	–	–
	XIV	22.37 ± 0.45	106.20 ± 6.14	–	–
	TCR-HA <sup>+/-</sup> /RIP-HA <sup>+/-</sup> mice	II	–	–	–
III		–	–	–	0.47 ± 0.13
IV		12.15 ± 1.42	323.78 ± 57.41	726.24 ± 60.32	0.36 ± 0.04
V		14.08 ± 2.34	331.30 ± 65.50	524.74 ± 42.20	–
VI		14.26 ± 1.27	423.63 ± 43.39	815.72 ± 70.24	–
VII		15.34 ± 1.83	410.86 ± 56.68	848.13 ± 51.01	–
VIII		15.65 ± 1.37	464.47 ± 41.93	891.61 ± 69.30	–
IX		16.77 ± 1.81	489.86 ± 52.26	935.08 ± 58.04	–
X		17.80 ± 2.34	523.30 ± 58.57	889.01 ± 33.10	–
XI		20.82 ± 1.79	552.00 ± 64.10	999.90 ± 0.00	–
XII		20.46 ± 1.79	563.00 ± 61.89	870.21 ± 74.15	–
XIII		20.93 ± 1.93	541.06 ± 67.70	967.17 ± 26.73	–
XIV		20.75 ± 2.37	543.93 ± 63.24	999.90 ± 0.00	–

## ACTION POTENTIAL CHARACTERISTICS IN DIABETIC CONDITIONS

Some studies on the development of type II diabetes in Zucker diabetic fatty rats, upon 10 weeks of hyperglycemic condition, demonstrate that the action potentials in sensory neurons were reduced and the sensorial conduction velocity is slowed (distal > proximal) [25].

In our study, we have investigated the action potential in sensory neurons from dorsal root ganglia dissected from TCR-HA<sup>+/-</sup>/RIP-HA<sup>+/-</sup> mice. We have recorded the action potential in medium and large neurons in genetic-induced diabetes and in normoglycemic conditions. The classification of neurons was done by considering their capacities, according to Gao *et al.* [10], into three groups: small ( $\leq 29$  pF), medium-sized (30–69 pF), and large ( $\geq 70$  pF) neurons.

We have monitored the action potential amplitude and duration, both for the conventional mice and for the double transgenic mice. The amplitude of the action potential decreases significantly in diabetic conditions (Fig. 2). This fact is in agreement with the decrease in amplitude recorded for the female Zucker Diabetic Fatty (ZDF) rat [25], which is a good model for neuropathy development in type II diabetes animals. In our genetic model (TCR-HA<sup>+/-</sup>/RIP-HA<sup>+/-</sup>), we might suppose that the neuropathy is already installed and after 10 weeks of hyperglycemia, the same sensory nerve excitability decrease is recorded. In clinics, patients that are accusing neuropathic pain are experiencing a slowing in the action potential velocity, which is correlated with the rate and kind of nerve fiber degeneration [7]. At the molecular level, this phenomenon can be explained by an enhanced tendency of protein glycosylation in the neurons [15]. In patients with distal sensory neuropathy, nerve action potential amplitudes of sural and superficial peroneal nerves decreased compared to healthy patients [28]. In our study, the nerve fiber degeneration induces a reduction of the action potential amplitude (Fig. 2).

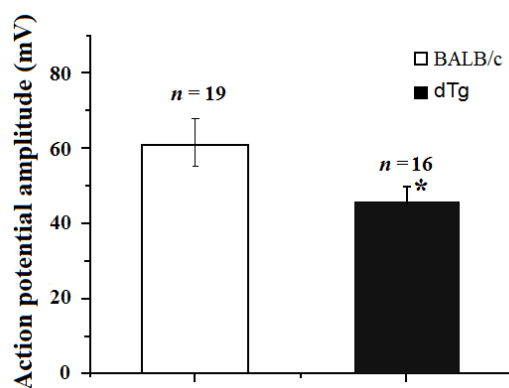


Fig. 2. Action potential amplitude in BALB/c and TCR-HA<sup>+/-</sup>/RIP-HA<sup>+/-</sup> mice.

Another important characteristic of the action potential which was considered is the phase duration. Different physiological mechanisms are involved in the evolution of the action potential phases, such as opening of the voltage-gated sodium channels (during the depolarization phase), inactivation and closing of the voltage-gated sodium channels, opening of the delayed-rectified voltage-gated potassium channels, increased activity of the Na<sup>+</sup>-K<sup>+</sup> pump (during the repolarization phase) and opening of the I<sub>h</sub> channels (during the post-hyperpolarization phase). All these proteins (i.e. ion channels, pumps, etc.) are direct targets during the glycosylation process initiated by the hyperglycemic condition installed in TCR-HA<sup>+/-</sup> / RIP-HA<sup>+/-</sup> mice.

The duration of the depolarization phase is not affected in diabetic mice compared to normal mice (Fig. 3A). This can be explained by the fact that the activation constant of the voltage-gated sodium channels is not modified by hyperglycemia. Other speculations might include the idea that the mean opening time of the voltage-gated sodium channels is not modified in diabetic conditions. Beside these theories, one should take into account that there are several voltage-gated sodium channel types expressed in the sensory neurons (some of them being tetrodotoxin-resistant and others being tetrodotoxin-sensitive), and their kinetics and structure might be distinctly affected by glycosylation processes.

The duration of the repolarization phase is prolonged for the diabetic mice compared with conventional mice (Fig. 3B). It should be taken into account that the metabolic rate of the neurons is strongly affected by diabetes, and the fact is closely related with the decreased production of ATP. Consequently, this modification in the repolarization phase duration might be attributed to a decrease in the Na<sup>+</sup>-K<sup>+</sup>-ATPase rate cycle. In conclusion, the total action potential duration (Fig. 3C) is statistically significant more prolonged in diabetic conditions.

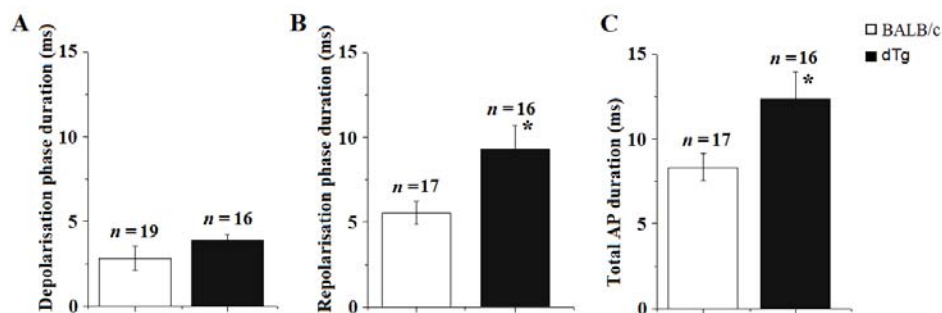


Fig. 3. Action potential phase duration for BALB/c mice vs. TCR-HA<sup>+/-</sup>/RIP-HA<sup>+/-</sup> mice. A. Depolarisation phase duration. B. Repolarisation phase duration. C. Total action potential (AP) duration.

### $I_h$ CURRENT CHARACTERISTICS IN DIABETIC CONDITION

The current  $I_h$  is defined through HCN channels (hyperpolarization-activated cyclic-nucleotide-gated channels). It is a non-selective cationic current, that is activated by the membrane hyperpolarization and that appears at the end of the action potential. Stimuli which may modulate the  $I_h$  characteristics are: inflammatory mediators, increased intracellular cAMP, changes in membrane voltage and the hypoxia condition [10, 13, 29].  $I_h$  currents are involved in the generation and frequency of the spontaneous activity for the rat CNS and the rat dorsal root ganglia neurons, but there can also be found in the autonomous cardiac system.

In type I diabetes, there is a dysfunction of the arterial baroreflex, this fact being attributed to the influence of HCN channels on the decrease in AB neurons excitability (aortic baroreceptors from nodous nucleus). Indeed, the blockage of HCN channels by cesium chloride or ZD-7288 determines a significant reduction in HCN currents and an increase of the action potential frequency for AB neurons from rats affected by streptozotocin-induced type I diabetes [13]. In addition, there are some studies on streptozotocin-induced diabetes that indicate a reduction of the inward rectification in motor axons [29], and this reduction potentiates conduction block caused by activity-dependent hyperpolarization. Peripheral block of  $I_h$  produces an antiallodynic effect, which suggests that  $I_h$  channels represent a novel target for nerve block treatment of postoperative and neuropathic pain [5].

In our study, we have evaluated the effect induced by genetic induced diabetes on the neurons excitability by means of mechanisms that involve the  $I_h$  currents. Two parameters have been monitored: the amplitude and the time constant of  $I_h$  currents. The amplitude of the hyperpolarization currents is not affected by diabetes (data not shown).

Data from literature indicate the presence in the dorsal root ganglia neurons of two different types of  $I_h$  currents: fast kinetics and slow kinetics [10]. We have recorded both current types in the neurons, in normal and diabetic conditions. The time dependence of  $I_h$  during the activation was fitted using an exponential equation, using the software Clampfit 9.0. For some sensory neurons,  $I_h$  was best fitted by a single exponential equation of the following form:

$$I_{h(t)} = A(1 - e^{-(t/\tau_F)}) + C \quad (1)$$

and for other neurons the best fit was done with a double exponential equation

$$I_{h(t)} = A_1(1 - e^{-(t/\tau_F)}) + A_2(1 - e^{-(t/\tau_S)}) + C \quad (2)$$

where  $\tau_S$  and  $\tau_F$  were the fast and slow time constants, respectively. The classification was done considering that fast kinetics currents have  $\tau_F < 350$  ms and slow kinetics currents have  $\tau_S > 350$  ms [10]. In Eq. 1 and Eq. 2, the constant  $\tau_F$  has the same meaning and the same range of values. When plotting the Fig. 4A, all the constants  $\tau_F$ , from the single and double exponential fit, were reunited.

$\tau_F$  (at  $-80$  mV) does not present any significant differences between diabetic mice and normal mice (Fig. 4A). Instead,  $\tau_S$  (at  $-80$  mV) has a significant increase in diabetic conditions (Fig. 4A).

$I_h$  currents are implied in the autonomous discharge rate of the action potentials in the heart and brain. In particular,  $I_h$  in sensory neurons modulates the action potential frequency and has a direct correlation with the neuronal excitability properties. In diabetes, the excitability is profoundly affected, the refractory period being increased, and implicitly we expect an active role of the slow kinetics  $I_h$  currents. Thus, the increase of  $\tau_S$  is well correlated with the development of neuropathic condition in hyperglycemic state.

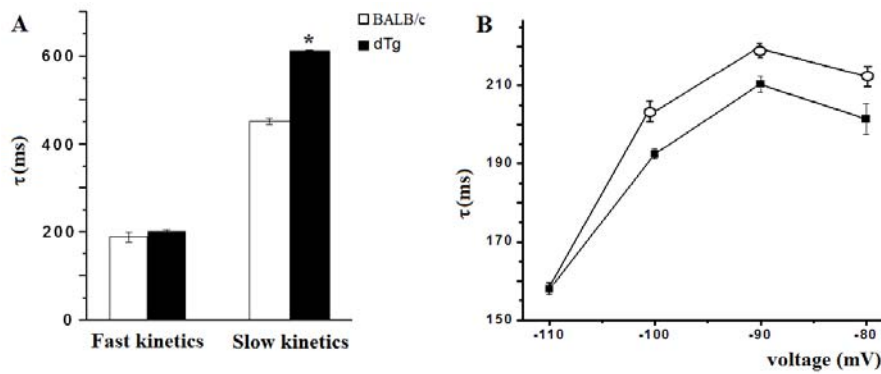


Fig. 4. A. The time constants of the hyperpolarization current for the fast- and slow- kinetics neurons at  $-80$  mV. The time constant of neurons with slow kinetics is significantly higher for TCR- $HA^{+/-}$ /RIP- $HA^{+/-}$  vs BALB/c mice. B. The mean time constant for fast kinetics neurons (best fitted with a single exponential equation) vs. test membrane potential. The squares represent data for BALB/c mice ( $n = 14$ ) and the circles for TCR- $HA^{+/-}$ /RIP- $HA^{+/-}$  mice ( $n = 8$ ).

The mean time constant for fast kinetics neurons was plotted against the test membrane potential, and we have observed a shift of the  $\tau_F$  to higher values for TCR- $HA^{+/-}$ /RIP- $HA^{+/-}$  mice compared to BALB/c mice (Fig. 4B). This tendency might be explained by the fact that diabetic condition determines an increase of the number of neurons with slow kinetics, even though this shift does not generate a jump from the fast kinetics category to the slow one. It is important to highlight that despite the lack of differences of  $\tau_F$  (at  $-80$  mV) in diabetic vs. normal conditions (Fig 4A), a significant modification of mean time constant can be detected when we plot it for different membrane voltage values (Fig. 4B).

A simple approach allowed us to evaluate the number of neurons with fast kinetics ( $N_F$ ) and slow kinetics ( $N_S$ ) with respect to the total number of neurons ( $N_T$ ) that expressed the  $I_h$  currents (Table 2). It is important to mention that only 75 % of tested neurons expressed  $I_h$  currents.

Table 2

Percentage of sensory neurons with fast and slow kinetics from the dorsal root ganglia of dTg mice vs normal mice

	$N_F / N_T$	$N_S / N_T$
BALB/c mice	14 / 18 (77.78 %)	4 / 18 (22.22 %)
TCR-HA <sup>+/-</sup> /RIP-HA <sup>+/-</sup> mice	8 / 14 (57.14 %)	6 / 14 (42.86 %)

In BALB/c mice,  $N_F$  is approximately 3.5 times more elevated than  $N_S$  (Table 1). In TCR-HA<sup>+/-</sup>/RIP-HA<sup>+/-</sup> mice,  $N_F$  is almost equal to  $N_S$ . A general appreciation involves that the level of expression of  $I_h$  is dramatically affected by the diabetic condition, and that the level of expression of slow kinetics  $I_h$  channels is increased by hyperglycemia. This fact might be correlated with the increase of  $\tau_S$  in TCR-HA<sup>+/-</sup>/RIP-HA<sup>+/-</sup> mice.

## CONCLUSIONS

Considering all the electrophysiological reported data, we can draw the following conclusions related to the hyperglycemic condition: (i) the action potential amplitude is reduced; (ii) the total action potential duration is prolonged due to the increase of the repolarization phase; (iii) fast kinetics  $I_h$  currents do not have a significant modification of the time constant at  $-80$  mV, but the general voltage profile is shifted towards higher values; (iv) slow kinetics  $I_h$  currents have a significant increase of the time constant at  $-80$  mV; (v) the balance in the level of  $I_h$  expression is bending to the slow kinetics currents.

The complicated kinetics of  $I_h$  activation may reflect the presence of multiple isoforms of the  $I_h$  channel. Four members of a gene family encoding mammalian HCN channels (HCN1–HCN4) have been cloned in recent years. In addition, the distribution pattern of  $I_h$  varies with the size of mouse DRG neurons [10]. Further studies should be done by RT-PCR in order to evaluate the level of expression of each HCN isoform. These data could be supplemented with single-channel recordings by patch-clamp techniques, with a proper usage of pharmacological inhibitors of different HCN isoforms.

Previous studies have pointed out that TCR-HA<sup>+/-</sup>/RIP-HA<sup>+/-</sup> mice model is prone to describe the cardiovascular and renal features of type I diabetes [22]. In addition, our mouse model is well suited for the description of certain characteristics encountered in diabetic neuropathy, such as nerve damage. Clinical data of decreased action potential velocity are correlated with our recordings at the cellular level. Thus, this model can be used for further investigation of the diabetic condition, and in particular to test improved pharmacological treatments.

*Acknowledgment.* This work was supported by the grant PNCDI2 41-074/2007 of the Romanian Ministry of Research.

## REFERENCES

1. AHLGREN, S.C., J.F. WANG, J.D. LEVINE, C-fiber mechanical stimulus-response functions are different in inflammatory versus neuropathic hyperalgesia in the rat, *Neuroscience*, 1997, **76**, 285–290.
2. APOSTOLOU, I., H. VON BOEHMER, The TCR-HA, INS-HA transgenic model of autoimmune diabetes: limitations and expectations, *J. Autoimmun.*, 2004, **22**, 111–114.
3. ANAND, P., G. TERENGI, G. WARNER, P. KOPELMAN, R.E. WILLIAMS-CHESTNUT, D.V. SINICROPI, The role of endogenous nerve growth factor in human diabetic neuropathy, *Nat. Med.*, 1996, **2**, 703–707.
4. BOULTON, A.J., R.A. MALIK, Diabetic neuropathy, *Med. Clin. North Am.*, 1998, **82**, 909–929.
5. DALLE, C., J.C. EISENACH, Peripheral block of the hyperpolarization-activated cation current (I<sub>h</sub>) reduces mechanical allodynia in animal models of postoperative and neuropathic pain, *Reg. Anesth. Pain Med.*, 2005, **30**(3), 243–248.
6. DI MARZO, V., P.M. BLUMBERG, A. SZALLASI, Endovanilloid signaling in pain, *Curr. Opin. Neurobiol.*, 2002, **12**, 372–379.
7. DYCK, P.J., E.H. LAMBERT, P.C. O'BRIEN, Pain in peripheral neuropathy related to rate and kind of fiber degeneration, *Neurology*, 1976, **26**, 466–471.
8. DICKENSON, A.H., E.A. MATTHEWS, R. SUZUKI, Neurobiology of neuropathic pain: mode of action of anticonvulsants, *Eur. J. Pain*, 2002, **6**, A51–A60.
9. FOX, A., C. EASTWOOD, C. GENTRY, D. MANNING, L. URBAN, Critical evaluation of the streptozotocin model of painful diabetic neuropathy in the rat, *Pain*, 1999, **81**, 307–316.
10. GAO, L.L., Y.L. SONG, M. TANG, C.J. LIU, X.W. HU, H.Y. LUO, J. HESCHELER, Effect of hypoxia on hyperpolarization-activated current in mouse dorsal root ganglion neuron, *Brain Res.*, 2006, **1078**, 49–59.
11. HIRADE, M., H. YASUDA, M. OMATSU-KANBE, R. KIKKAWA, H. KITASATO, Tetrodotoxin-resistant sodium channels of dorsal root ganglion neurons are readily activated in diabetic rats, *Neuroscience*, 1999, **90**, 933–939.
12. HONG, S., J.W. WILEY, Early painful diabetic neuropathy is associated with differential changes in the expression and function of vanilloid receptor 1, *J. Biol. Chem.*, 2005, **280**, 618–627.
13. LI, Y.L., T.P. TRAN, R. MUELLEMAN, H.D. SCHULTZ, Blunted excitability of aortic baroreceptor neurons in diabetic rats: involvement of hyperpolarization-activated channel, *Cardiovasc. Res.*, 2008, **79**(4), 715–721.
14. KAMEI, J., K. ZUSHIDA, K. MORTIA, M. SASAKI, S. TANAKA, Role of vanilloid VR1 receptor in thermal allodynia and hyperalgesia in diabetic mice, *Eur. J. Pharmacol.*, 2001, **422**, 83–86.
15. KAPUR, D., Neuropathic pain and diabetes, *Diabetes Metab. Res. Rev.*, 2003, **19**, S9–S15.
16. KIHARA, M., J.D. SCHMELZER, J.F. PODUSLO, G.L. CURRAN, K.K. NICKANDER, P.A. LOW, Aminoguanidine effects on nerve blood flow, vascular permeability, electrophysiology, and oxygen free radicals, *Proc Natl Acad Sci USA.*, 1991, **88**(14), 6107–6111.
17. LEE, Y.H., T.G. RYU, S.J. PARK, E.J. YANG, B.H. JEON, G.M. HUR, K.J. KIM, Alpha 1-adrenoceptors involvement in painful diabetic neuropathy: a role in allodynia, *Neuroreport.*, 2000, **11**, 1417–1420.
18. MALCANGIO, M., D.R. TOMLINSON, A pharmacologic analysis of mechanical hyperalgesia in streptozotocin/diabetic rats, *Pain*, 1998, **76**, 151–157.
19. MAKINO, S., K. KUNIMOTO, Y. MURAOKA, Y. MIZUSHIMA, K. KATAGIRI, Y. TOCHINO, Breeding of a non-obese, diabetic strain of mice, *Jikken Dobutsu*, 1980, **29**(1), 1–13.
20. MANNION, R.J., C.J. WOOLF, Pain mechanisms and management: a central perspective, *Clin. J. Pain*, 2000, **16**, S144–S156.

21. MARLISS, E.B., A.F. NAKHOODA, P. POUSSIER, A.A.F. SIMA, The diabetic syndrome of the 'BB' Wistar rat: possible relevance to type 1 (insulin-dependent) diabetes in man, *Diabetologia*, 1982, **22**, 225–232.
22. RADU, D.L., A. GEORGESCU, C. STAVARU, A. CARALE, D. POPOV, Double transgenic mice with type 1 diabetes mellitus develop somatic, metabolic and vascular disorders, *J. Cell Mol. Med.*, 2004, **8**(3), 349–358.
23. RADU, D.L., N. NOBEN-TRAUTH, J. HU-LI, W.E. PAUL, C.A. BONA, A targeted mutation in the IL-4Ra gene protects mice against autoimmune diabetes, *Proc. Natl. Acad. Sci. USA*, 2000, **97**(23), 12700–12704.
24. ROMAN, L.M., L.F. SIMONS, R.E. HAMMER, J.F. SAMBROOK, M.-J.H. GETHING, The expression of influenza virus hemagglutinin in the pancreatic  $\beta$  cells of transgenic mice results in autoimmune diabetes, *Cell*, 1990, **61**, 363–396.
25. RUSSELL, J.W., A. BERENT-SPILLSON, A.M. VINCENT, C.L. FREIMANN, K.A. SULLIVAN, E.L. FELDMAN, Oxidative injury and neuropathy in diabetes and impaired glucose tolerance, *Neurobiol. Dis.*, 2008, **30**(3), 420–429.
26. SWINDLE, M.M., R.J. ADAMS, *Experimental Surgery and Physiology: Induced Animal Models of Human Disease*, Lippincott Williams & Wilkins, USA, 1988.
27. SUGIMOTO, K., Y. MURAKAWA, A.A. SIMA, Diabetic neuropathy a continuing enigma. *Diabetes Metab. Res. Rev.*, 2000, **16**, 408–433.
28. ULUC, K., B. ISAK, D. BORUCU, C.M. TEMUCIN, Y. CETINKAYA, P.K. KOYTAK, T. TANRIDAG, O. US, Medial plantar and dorsal sural nerve conduction studies increase the sensitivity in the detection of neuropathy in diabetic patients, *Clin Neurophysiol.*, 2008, **119**(4), 880–885.
29. YANG, Q., R. KAJI, T. TAKAGI, N. KOHARA, N. MURASE, Y. YAMADA, Y. SEINO, H. BOSTOCK, Abnormal axonal inward rectifier in streptozotocin-induced experimental diabetic neuropathy, *Brain*, 2001, **124**, 1149–1155.